

# Quantum Coherence Beyond the Thermal Length

S. E. J. Shaw

*Department of Physics, Harvard University, Cambridge, Massachusetts 02138, USA*

R. Fleischmann

*Max-Planck Institut für Strömungsforschung, Bunsenstraße 10, D-37073 Göttingen, Germany*

E. J. Heller

*Department of Physics and Department of Chemistry and Chemical Biology,  
Harvard University, Cambridge, Massachusetts 02138, USA*

(Dated: November 13, 2018)

Recent experiments have used scattering to map the flow of electrons in a two-dimensional electron gas. Among other things, the data from these experiments show perseverance of regular interference fringes beyond the kinematic thermal length. These fringes are seen in full quantum-mechanical simulations with thermal averaging, and within the phase coherence length they can also be understood with a simple, single-scattering model. This effect provides a new way to gauge the coherence length independent of thermal broadening. Appealing to higher-order scattering, we present a mechanism by which interference fringes may survive even beyond the phase coherence length.

## I. INTRODUCTION

In recent experiments, the flux of electrons through a quantum point contact (QPC) and into the bulk of a two-dimensional electron gas (2DEG) was probed with a charged atomic force microscope (AFM) tip [1, 2]. The tip, capacitively coupled to the 2DEG, created a movable scatterer of the electrons propagating through the system [3]. The measurements taken were of the conductance as a function of the position of the AFM tip above the sample. In the measurements, fringes spaced at half of the Fermi wavelength and oriented transverse to the electron flux were seen.

Close to the QPC, we can understand these interference fringes as arising from an open Fabry-Pérot cavity between the tip and the QPC. However, simple kinematic considerations suggest that these fringes should die out at some distance from the QPC, as waves that differ in energy drift out of phase with one another. In the experimental system, for example, waves differing in energy by  $kT$  drift out of phase by one radian over a round-trip distance of approximately 1300 nm. The fringes seen experimentally, however, survive well beyond this range.

The interference fringes beyond this thermal length are seen in full quantum-mechanical simulations with thermal averaging, as shown in Fig. 1, so we know that a complete theory reproduces them. This solution, however, doesn't tell us much about the mechanism that allows the fringes to survive. We present here a simple model, appealing only to first-order scattering, that shows that the fringes should survive up to the phase coherence length. Another mechanism for qualitatively different fringes *beyond* the coherence length is also presented; to date, experiments have not probed this regime.

The potential seen by electrons in a 2DEG is fundamental to the model presented here. As reported in [2], we have considered two contributions to this potential:

impurities and donor atom density fluctuations [4, 5]. The contribution of the donor atoms results in a random potential whose peaks lie well below the energy of the electrons, and thus are not expected to backscatter significantly. The impurities, on the other hand, are occasionally located close to the 2DEG and thus produce strong, localized scattering centers. It is these impurity scatterers that we will consider in our models below.

## II. SINGLE SCATTERING

Here we use a simple, first-order model to explain the fringes seen beyond the thermal length. The result requires phase coherent transport at each energy, and therefore does not apply beyond the phase coherence length. This mechanism was previously mentioned in [2], without the necessary details presented here, to establish priority.

### A. Thermal averaging

The thermal average is found by an integral over energy with the derivative of the Fermi function as a weighting function. In order to simplify the mathematics of this model, we seek an approximation that is an integral over wave vector with Gaussian weighting. For the ranges of parameters in this system, such an approximation can be made to an acceptable degree of accuracy. Typical values taken from the experiments, for example, give us a temperature of 1.7 K and a Fermi energy of 16 meV.

The thermal distribution of energies begins with the derivative of the Fermi function at the known temperature  $T$  and Fermi energy  $E_F$ . We find that

$$-f'(E) = \left[1 + e^{(E-E_F)/kT}\right]^{-2} \frac{1}{kT} e^{(E-E_F)/kT}$$

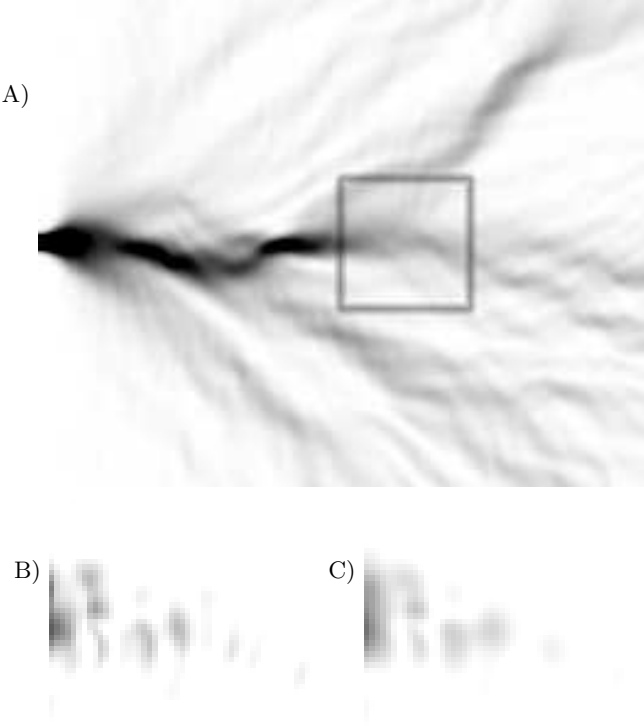


FIG. 1: Here we see the survival of interference fringes beyond the thermal length in a full quantum-mechanical simulation. (A) shows the quantum-mechanical flux through a system with a QPC and a disordered background; for a discussion of the “branched” nature of the flux, see [2]. In (B) we show the results of a “tip scan”, i.e. conductance change as a function of AFM tip position, at a fixed energy. The scan is performed in the indicated area of (A). In (C) we show the thermally averaged tip scan data in the same region. The temperature for the average was set such that the scan region is two thermal lengths from the QPC.

$$\approx \frac{1}{4kT} e^{-[(E-E_F)/(4kT\pi^{-1/2})]^2} \quad (1)$$

$$\approx \frac{1}{4kT} e^{-(k-k_0)^2 \ell_T^2}. \quad (2)$$

The standard deviation of the Gaussian in Eq. (1) was chosen to match both the value of  $-f'(E)$  at  $E = E_F$  and its approximate width; we can do both while preserving normalization. In Eq. (2) we have defined our kinematic thermal length  $\ell_T$  as

$$\ell_T = \hbar^2 k_0 \pi^{1/2} / 4mkT. \quad (3)$$

This is half the distance (since we are interested in round-trips) that it takes two waves separated in energy by the standard deviation of the Gaussian in Eq. (1) to drift one radian out of phase. This then is the weighting function that we will use in performing the thermal average.

Using Eq. (2) we will integrate over  $k$  rather than  $E$  in taking the thermal average. Given the dispersion relation  $E = \hbar^2 k^2 / 2m$ , we have  $dE = (\hbar^2 k / m) dk$ . Appealing to the physical values that will appear for  $k_0$

and  $\ell_T$ , over the range of the weighting function we can approximate this dispersion relation as linear and take  $dE = (\hbar^2 k_0 / m) dk$ . Hence for a signal  $s(k, r)$  at fixed wave vector, we have the thermally averaged signal  $s(r)$  given by

$$s(r) = \int \left( \frac{\hbar^2 k_0}{m} dk \right) \frac{1}{4kT} e^{-(k-k_0)^2 \ell_T^2} s(k, r) \quad (4)$$

$$= \pi^{-1/2} \ell_T \int dk e^{-(k-k_0)^2 \ell_T^2} s(k, r). \quad (5)$$

## B. The single scattering model

This model is quite simple. We take a random distribution of s-wave scatterers in a plane at the points  $\{\vec{r}_i\}$  and with scattering lengths  $\{a_i\}$ . We assume phase coherent transport over the round-trip distances. Furthermore, we make the following approximations, which have no effect on the qualitative results and little effect on the quantitative results: we use  $r^{-1/2} e^{ikr}$  rather than Bessel functions for the two-dimensional s-waves, assume for each scatterer a scattering amplitude proportional to the scattering length, and assume a phase shift equal to the scattering length times the wave number. The quantity of interest is the reduction of flux through the point contact as a result of the scattering.

We take the QPC to have at least one channel open, and in the single-scattering picture neglect backscattering from the point contact. Any conductance oscillations are then not due to interference of the returning amplitude with the outgoing amplitude, but rather result from interference of different ways of returning to the QPC. This is easily seen by considering an outgoing wave  $\exp[ikx]$  added to a backscattered wave  $\epsilon \exp[-ikx + \delta(r)]$  in the wire, where  $\delta(r)$  is the phase shift due to a backscattering obstruction at position  $r$ . It is readily seen that the net flux is independent of  $\delta$ , meaning one source of backscattering does not give fringes in conductance measurements.

Let the wave from the QPC be  $r^{-1/2} e^{ikr}$ , and the scattered wave from a point scatterer, measured at the QPC, be  $(ca_i/r_i) e^{ik(2r_i+a_i)}$ . The constant of proportionality between the scattering length and amplitude,  $c$ , depends on details of the scattering potentials irrelevant to this model. There are two factors of  $r_i^{-1/2}$ , one for the falloff of the wave illuminating the scatterer and one for the falloff of the scattered wave. The phase advances by the round-trip distance plus the phase shift. Let the tip be at a radius  $r_t$  and have the scattering length  $a_t$ , giving a similar return wave. Finally, to simplify the notation, let  $r'_i \equiv r_i + a_i/2$ .

The full return wave at a single energy is

$$\sum_i \frac{ca_i}{r_i} e^{2ikr'_i} + \frac{ca_t}{r_t} e^{2ikr'_t}. \quad (6)$$

The absolute square of this wave, the interference of various return paths, is the signal we require. We concentrate

on the cross terms, which will give rise to the oscillations with  $r_t$ . The cross terms are

$$s(r_t, k) = 2 \operatorname{Re} \left[ \sum_i \frac{c^2 a_i a_t}{r_i r_t} e^{2ik(r'_i - r'_t)} \right]. \quad (7)$$

We thermally average this signal using Eq. (5). Averaging after the absolute square so that it is an incoherent sum, we have

$$s(r_t) = 2\pi^{-1/2} \ell_T \operatorname{Re} \left[ \int dk e^{-(k-k_0)^2 \ell_T^2} \times \sum_i \frac{c^2 a_i a_t}{r_i r_t} e^{2ik(r'_i - r'_t)} \right]. \quad (8)$$

Changing the order of summation and integration, performing the Gaussian integral, and taking the real part, we are left with

$$s(r_t) = 2 \sum_i \frac{c^2 a_i a_t}{r_i r_t} \cos[2k_0(r'_i - r'_t)] e^{-(r'_i - r'_t)^2 / \ell_T^2}. \quad (9)$$

What remains is a contribution to the signal from all scatterers that are within a thermal length of being the same distance from the QPC as is the tip. In this expression, there is nothing special about the condition  $r_t > \ell_T$ . The thermal length still plays a role in that it determines the width of the band around  $r'_t$  that contributes to the thermally averaged signal. Note that the fringes predicted by this model are at half the Fermi wavelength, as observed. Furthermore, the fringes will be oriented perpendicular to the direction of electron flow, also as observed.

In Fig. 2 we show some examples of  $s(r_t)$ . To make the signal easier to observe, we divide out the overall  $r^{-3/2}$  dependence of the signal strength. Eq. (9) shows a clear  $r^{-2}$  dependence, but has an additional, not so obvious factor of  $r^{1/2}$ . This additional factor is related to the radial dependence of the number of scatterers in our  $\ell_T$ -wide band and the expectation value of a random sum of cosines.

There are other coherence effects that survive thermal averaging, such as weak localization, where the interference of time-reversed paths leads to an increased backscattering rate [6]. In contrast, the single-scattering effect discussed here originates from the interference of distinct paths of similar length, which can either increase or suppress backscattering.

The derivation above assumed infinite coherence length; however, it is clear that this mechanism cannot operate past this length, since it depends on interference of coherent backscattered amplitude. The appearance (or disappearance) of these backscattering fringes can become a new experimental measure of the coherence length.

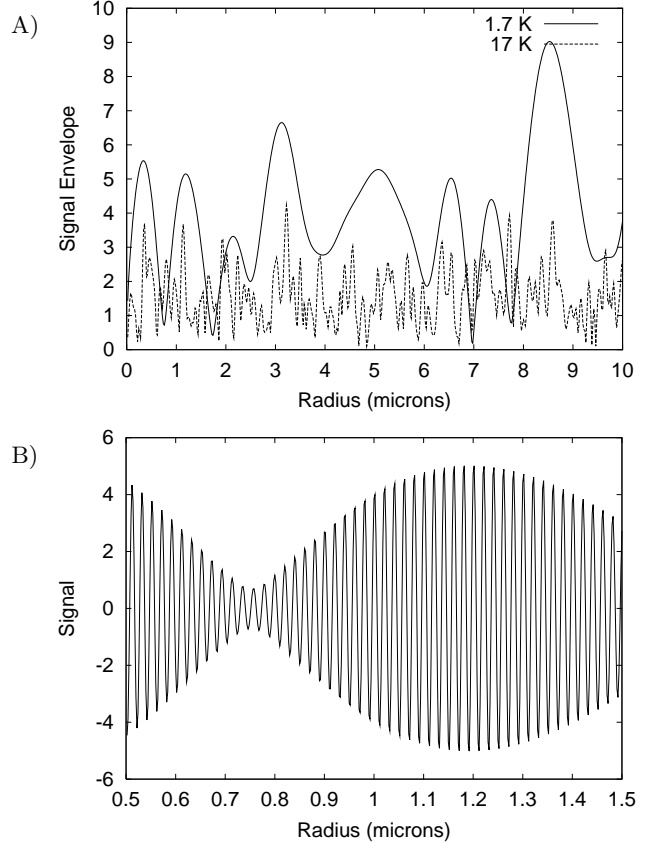


FIG. 2: Several examples of the signal generated by Eq. (9) with  $\lambda_0 = 40$  nm. In all cases, we have multiplied the data by  $r^{3/2}$ . In (A) we show the envelopes of two signals over a ten micron range; over this range, the oscillations under the envelopes would not be discernible in the figure. The two signals show the same random distribution of scatterers with a density of  $40 \mu\text{m}^{-2}$ , and differ only in their temperatures. We note that the increase in temperature results in a weaker signal with more rapid variation. In (B) we show the oscillatory signal under the envelope of the 1.7 K signal from (A), looking over a one micron range similar to that probed in experiments.

### C. Single scattering continuum limit

If we change the sum in Eq. (9) to an integral over the plane and let  $a_i = a \forall i$ , we go from a system of discrete scattering centers to a continuum approximation with constant density. We have

$$\begin{aligned} & \int_0^\infty dr \pi r \frac{2c^2 a a_t}{r r_t} \cos[2k_0(r' - r'_t)] e^{-(r' - r'_t)^2 / \ell_T^2} \\ &= \operatorname{Re} \left[ \int_0^\infty dr \frac{2\pi c^2 a a_t}{r_t} e^{2ik_0(r' - r'_t)} e^{-(r' - r'_t)^2 / \ell_T^2} \right] \quad (10) \\ &= \pi^{3/2} \ell_T \frac{c^2 a a_t}{r_t} e^{-k_0^2 \ell_T^2} \{1 + \\ & \quad \operatorname{Re} [\operatorname{erf}(ik_0 \ell_T + (r'_t - a/2)/\ell_T)]\}. \quad (11) \end{aligned}$$

The error function is oscillatory, but bounded in mag-

nitude. The dominant term for the magnitude of this signal is the exponential  $e^{-k_0^2 \ell_T^2}$ . For the values applicable in the physical systems that we have considered, this is vanishingly small; in this continuum limit, the signal disappears.

This implicit assumption of completely regular scatterer distribution isn't particularly justified, however. We already know from multiple scattering theory that such a regular distribution can appear as simply a mean field, effectively "raising the floor" of the potential over which the electrons propagate.

Even without this concern, this continuum limit calculation also tells us nothing about how that limit is approached. Simply taking the single-scattering model in Eq. (9) and increasing the density  $d$  of scatterers (without any correlation in their placement) reveals a  $d^{1/2}$  dependence of the signal strength. Clearly, however, at some density the single-scattering model ceases to be a useful one. A detailed study of how the infinite-order scattering calculations will cross over between domains is yet to be performed. The predictions of this model do hold, however, for infinite order scattering calculations with scatterer densities comparable to the experimental system. Preliminary results (Kalben et al.) indicate that the fringes are qualitatively similar even as multiple scattering becomes important.

### III. MULTIPLE SCATTERING

Just as simple kinematic considerations would lead one astray about the importance of the thermal length  $\ell_T$ , so

can one overestimate the importance of the phase coherence length  $\ell_\phi$ . Though the model described above depends on phase coherent transport, a resonance model predicts fringes of a qualitatively different nature at distances greater than  $\ell_\phi$ .

If the distance between the AFM tip and another scatterer is less than  $\ell_T$  and  $\ell_\phi$ , there can exist a resonance between the two. This resonance can increase or decrease the conductance through the full system despite incoherent transport over the distance back to the QPC. We are, in fact, quite accustomed to current carrying the signatures of resonance over great distances of incoherent transport, as this is the situation whenever we connect equipment to a 2DEG with room-temperature wires. This result is relatively easy to demonstrate in one dimension, using the transfer matrix formalism with dephasing built in.

The fringes generated by this resonance mechanism would not be centered on the QPC, but rather on the fixed scatterer participating in the resonance. This is the primary qualitative difference between this model and the single-scattering model proposed above. In the parameter ranges relevant to recent experiments (i.e., scatterer densities and tip ranges) we expect the single scattering mechanism to dominate.

- 
- [1] M. A. Topinka, B. J. LeRoy, S. E. J. Shaw, R. M. Westervelt, R. Fleischmann, E. J. Heller, K. D. Maranowski, and A. C. Gossard, *Science* **269**, 2323 (2000).
  - [2] M. A. Topinka, B. J. LeRoy, R. M. Westervelt, S. E. J. Shaw, R. Fleischmann, E. J. Heller, K. D. Maranowski, and A. C. Gossard, *Nature* **410**(6825), 183 (2001).
  - [3] M. A. Eriksson, R. G. Beck, M. Topinka, J. A. Katine, R. M. Westervelt, K. L. Campman, and A. C. Gossard, *Appl. Phys. Lett.* **69**, 671 (1996).
  - [4] J. H. Davies, *The Physics of Low-Dimensional Semiconductors* (Cambridge University Press, 1997).
  - [5] R. Grill and G. H. Döhler, *Physical Review B* **59**(16), 10769 (1999).
  - [6] P. Sheng, *Introduction to Wave Scattering, Localization, and Mesoscopic Phenomena* (Academic Press, 1995).